ARTICLE IN PRESS
+ MODEL

ELSEVIER

Journal of Structural Geology xx (2006) 1–16

JOURNAL OF STRUCTURAL GEOLOGY

www.elsevier.com/locate/jsg

Geomorphology and structure of the Jid right-lateral strike-slip fault in the Mongolian Altay mountains

R.T. Walker [a,*], A. Bayasgalan [b], R. Carson [c], R. Hazlett [d], L. McCarthy [e], J. Mischler [f], E. Molor [b], P. Sarantsetseg [b], L. Smith [g], B. Tsogtbadrakh [b], G. Tsolmon [b]

[a] *Department of Earth Sciences, University of Oxford, Parks Road, Oxford OX1 3PR, UK*
[b] *Geoinformatics Center, Mongolian University of Science and Technology, Ulaanbaatar, Mongolia*
[c] *Department of Geology, Whitman College, Walla Walla, WA, USA*
[d] *Department of Geology, Pomona College, Claremont, CA, USA*
[e] *Department of Geology, Colorado College, Colorado Springs, CO, USA*
[f] *Department of Geology, Augustana College, IL, USA*
[g] *Department of Geology, Princeton University, Princeton, NJ, USA*

Received 5 January 2006; received in revised form 13 April 2006; accepted 28 April 2006

Abstract

We describe the late Cenozoic structure and evolution of the Jid right-lateral strike-slip fault in the northern Mongolian Altay mountain chain. Parts of the Jid fault have a vertical component of motion, introduced by bending along the fault. Some locations show additional structural complexity at the Earth's surface, with parallel strands having strike-slip, normal and reverse faulting, probably indicating a spatial separation of dip-slip and strike-slip components of motion in cross-section. The Jid fault shows indications of recent movements at scales ranging from drainage re-organisation at the kilometre scale, to ground deformations likely to result from movements during the last earthquake, which occurred ~870–980 years ago based on OSL dating of deposits exposed in trenching. From the scale of the ruptures the earthquake would have had a magnitude of ~7.5 with an estimated right-lateral slip of ~5 m. Numerous horizontal offsets of about 10–15 m, and vertical scarps of ~5 m in the youngest alluvial deposits show the likely cumulative movement over the last ~15,000 years, and suggest a maximum slip-rate of roughly 1 mm/yr. The minimum cumulative right-lateral slip on the Jid fault is 1 km, which would accumulate in ~1 Ma at present-day rates of slip. The relatively small vertical component of motion on the Jid fault is not sufficient to generate topography in the adjacent Kharkhiraa and Türgen Uul mountains, with relief of over 2000 m. The high mountains may therefore result from localised uplift on thrust faults rather than by oblique slip on the Jid fault.

Keywords: Mongolia; Mongolian Altay; Strike-slip fault; Earthquake ruptures; Geomorphology

1. Introduction

Large strike-slip faults are an important feature of actively deforming parts of the continents, often reaching lengths of several hundreds of kilometres, and accumulating displacements of many kilometres. Such faults are capable of generating very large earthquakes such as the M_w 7.8 2001 Kunlun earthquake (e.g. Lin et al., 2002), and the M_w 7.9 2002 Denali earthquake in Alaska (e.g. Eberhart-Philips et al., 2003). The surface ruptures developed during large earthquakes provide a valuable constraint on the behaviour of seismogenic strike-slip faults. However, large earthquakes are relatively rare, and the ground deformations associated with earthquakes degrade rapidly due to erosion, thus limiting studies on large strike-slip faults and earthquakes to a rather limited set of examples.

* Corresponding author. Tel.: +44 1865 272013.
E-mail address: richw@earth.ox.ac.uk (R.T. Walker).

0191-8141/$ - see front matter © 2006 Elsevier Ltd. All rights reserved.
doi:10.1016/j.jsg.2006.04.007

Mongolia is a region of active faulting, and the potential for large strike-slip earthquakes is shown by the three great ($M > 8$) earthquakes in the country, and one in a nearby part of China, generated over the last century (Baljinnyam et al., 1993; see Fig. 1). In general, the historical records of earthquakes in Mongolia are poor. However, the landforms generated by individual slip events on faults in Mongolia are generally preserved to a very high degree due to the very low rates of erosion, allowing useful information to be gained from earthquake ruptures which are hundreds or potentially even thousands of years old (e.g. Khil'ko et al., 1985; Baljinnyam et al., 1993), information which is rapidly lost in most other actively deforming regions. In Mongolia, we can thus use the preservation of surface ruptures from pre-historic earthquake ruptures to extend the available record of events available for research into studies of large earthquakes. Cumulative offsets, resulting from repeated earthquakes, are also preserved to a high degree, and can often enable the estimation of long-term averaged slip-rates.

In this paper we describe, using field-based and remote sensing observations, the landscape in a tectonically active part of Mongolia for which we have no record of earthquakes. Our aims are to understand the slip behaviour, structure and evolution of the faulting, and also to help determine how tectonic strain is accommodated in this part of Asia. Preserved surface ruptures from a pre-historic event provide valuable additional constraints on the structure of the fault.

In the following sections, we first outline the tectonic setting, seismicity and geological history of the Mongolian Altay. We then describe in detail the geomorphology and structure of the Jid fault, a previously undescribed strand of the Tsagaan Shuvuut right-lateral fault system (sometimes referred to as the Har-Us-Nuur fault system, e.g. Tapponnier and Molnar, 1979; Cunningham et al., 1996; Cunningham, 2005). Our observations provide information on the behaviour of the fault during individual earthquakes, as well as the evolution of the fault over much longer timescales. Finally, we examine the significance of our results for the overall development of the Kharkhiraa mountains and the role of the Jid fault, and adjacent fault segments, in the accommodation of the regional tectonic strain. Although the Jid fault is only a relatively minor strand of the Tsagaan Shuvuut active fault system, its distinctive geomorphology and well-preserved earthquake ruptures provide much more information on the fault evolution than other, apparently more dominant, strands.

2. The Altay mountains: geology, seismicity and late Cenozoic tectonics

The active tectonics of Mongolia result from the Indo-Eurasian continental collision (e.g. Molnar and Tapponnier, 1975; Tapponnier and Molnar, 1979). Zones of active faulting and seismicity are concentrated in western parts of the country (e.g. Fig. 1). The NNW–SSE oriented Mongolian Altay mountains form the western border of the country and contain several parallel active right-lateral strike-slip faults, which have generated both historical and recent earthquakes, including the M_s 8.0 Fu Yun earthquake in 1931 (Baljinnyam et al., 1993), and more recently, an M_w 7.2 earthquake in the Russian Altay (Rogozhin et al., 2004). East of the Mongolian Altay lies the Hangay block, a region of high elevation, minor normal faulting and basaltic volcanism (Cunningham, 2000). The

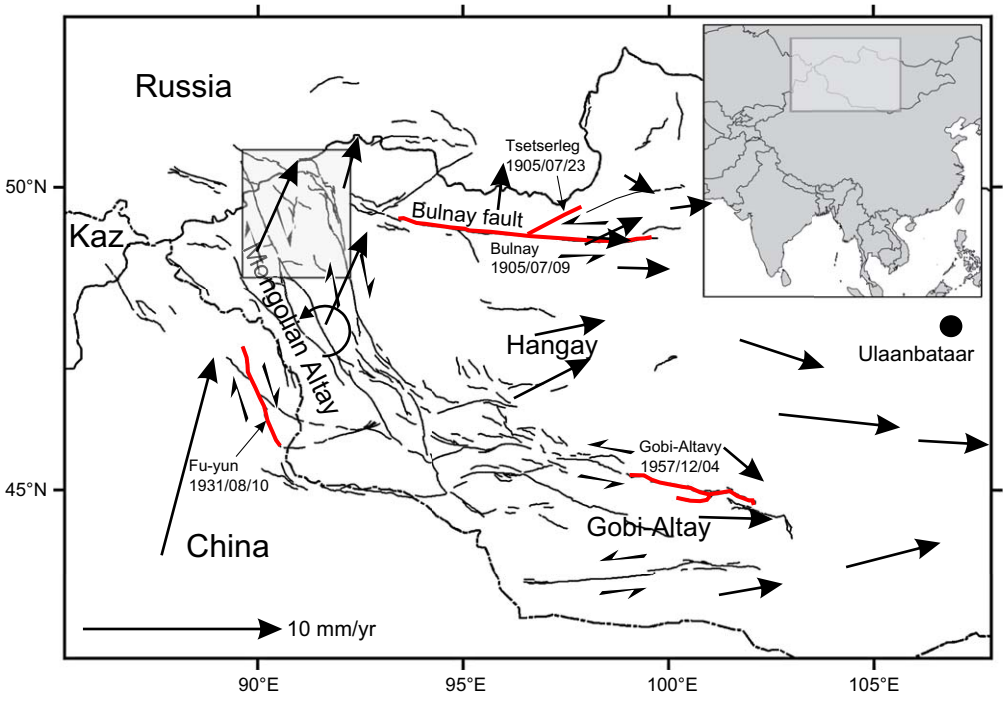

Fig. 1. Location map showing major active fault systems in western Mongolia. Thickened lines (red in online version) show ruptures of the four $M > 8$ earthquakes in the last century. Black arrows represent GPS velocities of points relative to Siberia (stable Eurasia) from Calais et al. (2003). The box shows the region represented in Fig. 2. This map is in a Mercator projection.

Hangay block is bordered to the south by the east–west Gobi–Altay left-lateral strike-slip fault system, which generated an M_s 8.3 earthquake in 1957 (e.g. Kurushin et al., 1997). To the north, the Hangay block is bordered by the east–west left-lateral Bulnay fault system, which generated two earthquakes of M_s 8.2 and 8.3 in the summer of 1905 (e.g. Baljinnyam et al., 1993).

The conjugate left- and right-lateral faulting in the Gobi–Altay and Mongolian Altay mountains is thought to accommodate shortening between western China and Siberia by vertical axis rotation of fault-bounded blocks (e.g. Baljinnyam et al., 1993). Recently published GPS measurements (shown in Fig. 1) show ~10 mm/yr of NNE directed shortening between China and Siberia (stable Eurasia), of which ~7 mm/yr is accommodated across the Mongolian Altay (Calais et al., 2005). From a comparison of earthquake slip-vector azimuths with the published GPS velocities, Bayasgalan et al. (2005) suggest that the Mongolian Altay must rotate anti-clockwise about a vertical axis in order for the faults to accommodate the regional velocity field. In contrast, both the GPS velocities relative to stable Eurasia and earthquake slip-vector azimuths in areas east of the Mongolian Altay are aligned east–west, and there is no requirement for the deformation in these regions to involve vertical axis rotation (Bayasgalan et al., 2005).

The geology of the Mongolian Altay mountains is composed mostly of amalgamated island-arc terranes, dating from the Palaeozoic (e.g. Cunningham et al., 1996; Badarch et al., 2002; Cunningham, 2005). The topography is characterised by a series of parallel NNW–SSE trending fault-bounded ranges, which reach elevations of over 4000 m in places. Regionally extensive peneplain surfaces are often preserved at mountain summits, suggesting that there was little regional relief prior to the Late Cenozoic reactivation (e.g. Cunningham et al., 2003). A rapid increase in coarse clastic sedimentation in the Miocene may date the onset of mountain building (e.g. Cunningham et al., 2003).

The known active faults in the Mongolian Altay tend to occur at the foot of the major ranges, and exploit pre-existing basement fabrics (Cunningham et al., 2003). The easternmost of the major strike-slip systems of the Altay is often referred to as the Har-Us-Nuur fault (e.g. Tapponnier and Molnar, 1979; Cunningham et al., 1996; Cunningham, 2005). In this paper, we follow the 1:1,000,000 scale Tectonic map of Mongolia (Tomurtogoo, 2002) in calling it the Tsagaan Shuvuut fault system. The Tsagaan Shuvuut fault roughly follows the eastern margin of the high mountainous topography (Fig. 2). In contrast to many of the Altay strike-slip faults, the Tsagaan Shuvuut fault system does not form a single structure at the base of the topographic slope. Instead, it breaks into a number of sub-parallel strands along the eastern margin of the glaciated Kharkhiraa and Türgen Uul massifs (Fig. 2), which reach elevations of over 4000 m. The Jid fault strand is the westernmost of the Tsagaan Shuvuut strands and is situated at elevations of ~2000 m to 2500 m. The Depression of Great Lakes, which runs along the eastern margin of the Altay mountains, forms the regional base level, with a typical elevation of ~1000–1500 m.

3. Structure and geomorphology of the Jid fault

The Jid fault and surrounding regions are shown in Fig. 3. Fault scarps within Quaternary deposits are seen along the entire length of the fault. South of the Burgastay river the Jid fault runs along the eastern margin of the north–south Jid hills, which are ~30 km long, with relief of ~300 m above the surrounding plains (Fig. 3B). Some small, and discontinuous, fault scarps can also be traced along the western margin of the range. Two ~1 km-wide elongate basins (the Horhoitiin Zaag and Tsagaan Nuur basins) bound the eastern side of the Jid hills (Fig. 3). North of the Burgastay river the fault cuts through relatively high topography. In the summer of 2004, we made detailed field observations along ~55 km of the Jid fault from its southern end to the Kharkhiraa river (between points X and Y in Fig. 3A). In the following sections, we first describe earthquake surface ruptures identified during our fieldwork (Section 3.1). We then describe, from north to south, landforms resulting from cumulative fault movements (Section 3.2). In Section 3.3, we estimate the slip-rate averaged over the last 10–15 ka, and use satellite imagery to determine the likely total cumulative displacement across the fault.

3.1. Description of surface ruptures

Fig. 4 shows photographs of surface ruptures along the Jid fault trace. The ruptures can be traced along most of the fault as a series of *en echelon* left-stepping tension cracks (e.g. Fig. 4B), and right-stepping push-up ridges or 'mole tracks' (Fig. 4A). The orientation of the mole tracks is consistent with predominantly right-lateral motion. In some localities the ruptures occur as single, or multiple, linear tracks extending for several hundreds of metres and trending parallel to the overall fault trace (e.g. Fig. 4C). The ruptures are closely associated with cumulative Late Quaternary scarps, which are described in detail in Section 3.2.

Alternating tension cracks and push-up ridges are commonly generated at the Earth's surface during strike-slip earthquakes and are likely to be underlain by a single seismogenic surface at depth (e.g. Lin et al., 2002). The partially infilled left-stepping tension cracks are easily identified in the field, as the dark green grass in the ruptures contrasts with the sparser vegetation growing on unbroken ground. The tension cracks are typically ~10–15 m long and 2–3 m wide, though some are up to 70 m long. Similarly, long tension fractures were observed along the 1905 Bulnay earthquake rupture, and are common elsewhere in Mongolia, and this style of rupturing may be influenced by freezing of the ground in the cold Mongolian climate (Baljinnyam et al., 1993). The Jid fault is located at elevations of ~2500 m, and periglacial landforms such as patterned ground and solifluction lobes are observed, suggesting that the ground is frozen along at least some parts of the fault.

We found relatively few indications of the amount of slip across the ruptures. The clearest offset is at 49°24′54.6N,

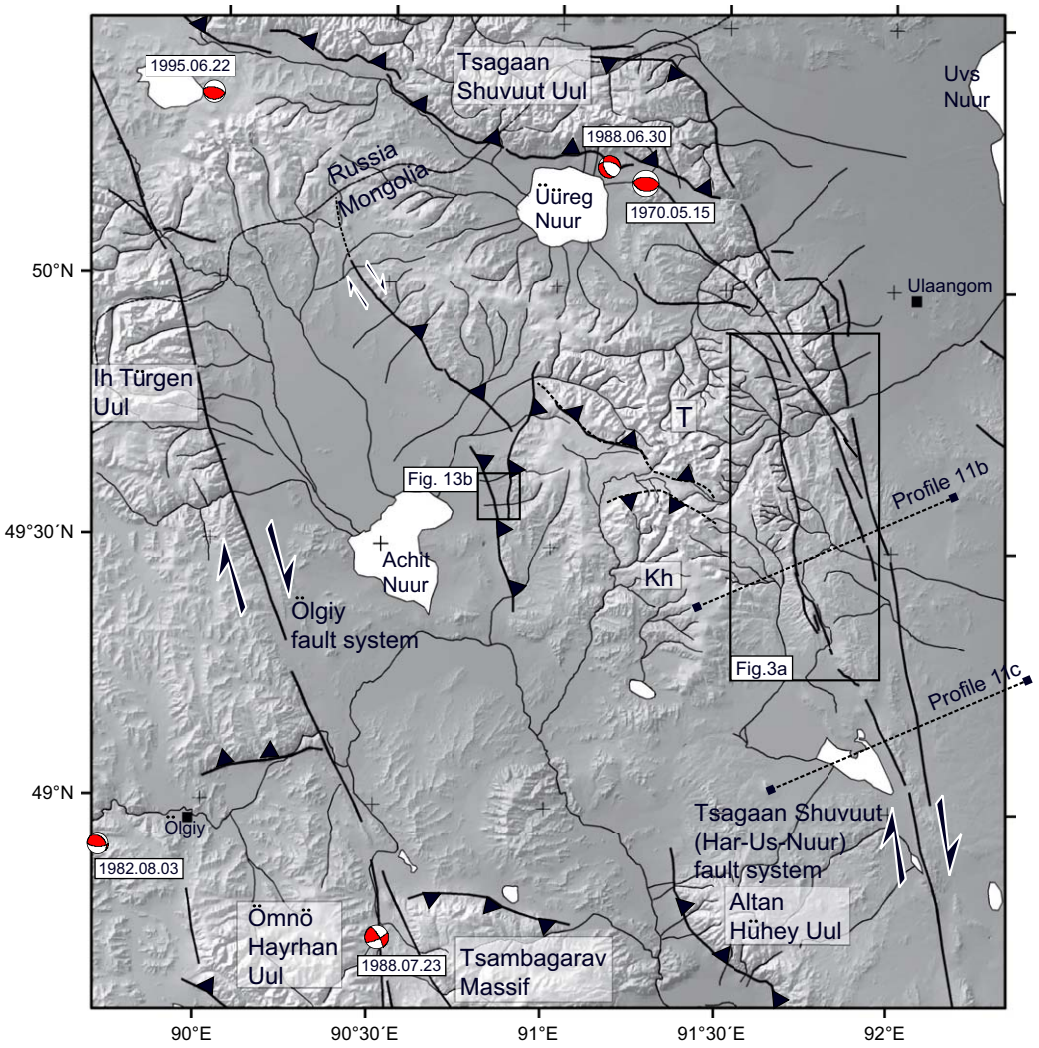

Fig. 2. Shaded relief SRTM (Shuttle-Borne Radar Topography Mission) topography (Farr and Kobrick, 2000) of the northern Mongolian Altay (see Fig. 1 for location). The NNW–SSE Ölgiy and Tsagaan Shuvuut right-lateral strike-slip faults cut across the image. In the south, isolated massifs (Ömnö Hayrhan Uul, Tsambagarav, and Altun Hühey Uul) occur at restraining bends on the strike-slip faults (e.g. Cunningham et al., 2003). The Tsagaan Shuvuut fault system is bounded to the west by the Türgen Uul (T) and Kharkhiraa (Kh) massifs, both of which reach elevations of over 4000 m and are glaciated. Fault-plane solutions for the 1970.05.15 Üüreg Nuur (M_w 6.3), the 1988.07.23 Tsambagarav (M_w 5.7), and the 1995.06.22 Tsagaan Shuvuut (M_w 5.4) earthquakes are from waveform modelling (Bayasgalan et al., 2005). The other two fault-plane solutions are from the Harvard CMT catalogue. Boxes show the regions represented in later figures. This, and all later maps, is in a UTM zone 46 projection.

91°44′42.5E (Fig. 4D), where a small stream shows displacement of ~3.2 m right-laterally, and ~20 cm vertically (up to the west). There are two parallel fault strands with earthquake ruptures at this latitude (Fig. 3; see also Section 3.2.2), so the total displacement across all strands should be greater. We found another possible, though not certain, stream offset of ~4.3 m at 49°30′49.7N, 91°42′48.6E. The width of the tension cracks themselves also provides an approximate idea of the amount of slip. The most reliable measurements of extension are made where individual features can be correlated across the tension cracks. In Fig. 5 we correlated sharp bends in the trace of the tension crack to measure opening of ~3.2–6.6 m in a direction parallel to the local trend of the fault.

The ratio of the amount of slip in an earthquake over rupture length ($\overline{u}/L$), in earthquakes is found to be roughly constant, with a value of $\sim 5 \times 10^{-5}$ (e.g. Scholz, 1982). Assuming that the ~55 km of ruptures found along the Jid fault were generated in a single earthquake, the expected amount of slip would be ~2.7 m. The few unambiguously displaced streams and the scale of the ruptures themselves suggest amounts of slip of substantially more than 3 m. It is therefore probable, though not certain, that the earthquake ruptured more than the 55 km investigated in the field. The Jid fault can be traced on satellite imagery for ~90 km (Fig. 2). If the earthquake ruptured the entire 90 km fault length, it would generate slip of ~4.5 m (using the ratio of $\overline{u}/L = 5 \times 10^{-5}$), which is within the observed range. From the relationship $M_0 = \mu A \overline{u}$, we estimate a moment of $\sim 1.82 \times 10^{20}$ Nm for an earthquake rupturing the entire 90 km length of the fault. For these estimates we have assumed values of 3×10^{10} N/m for the shear modulus (μ) and a depth of

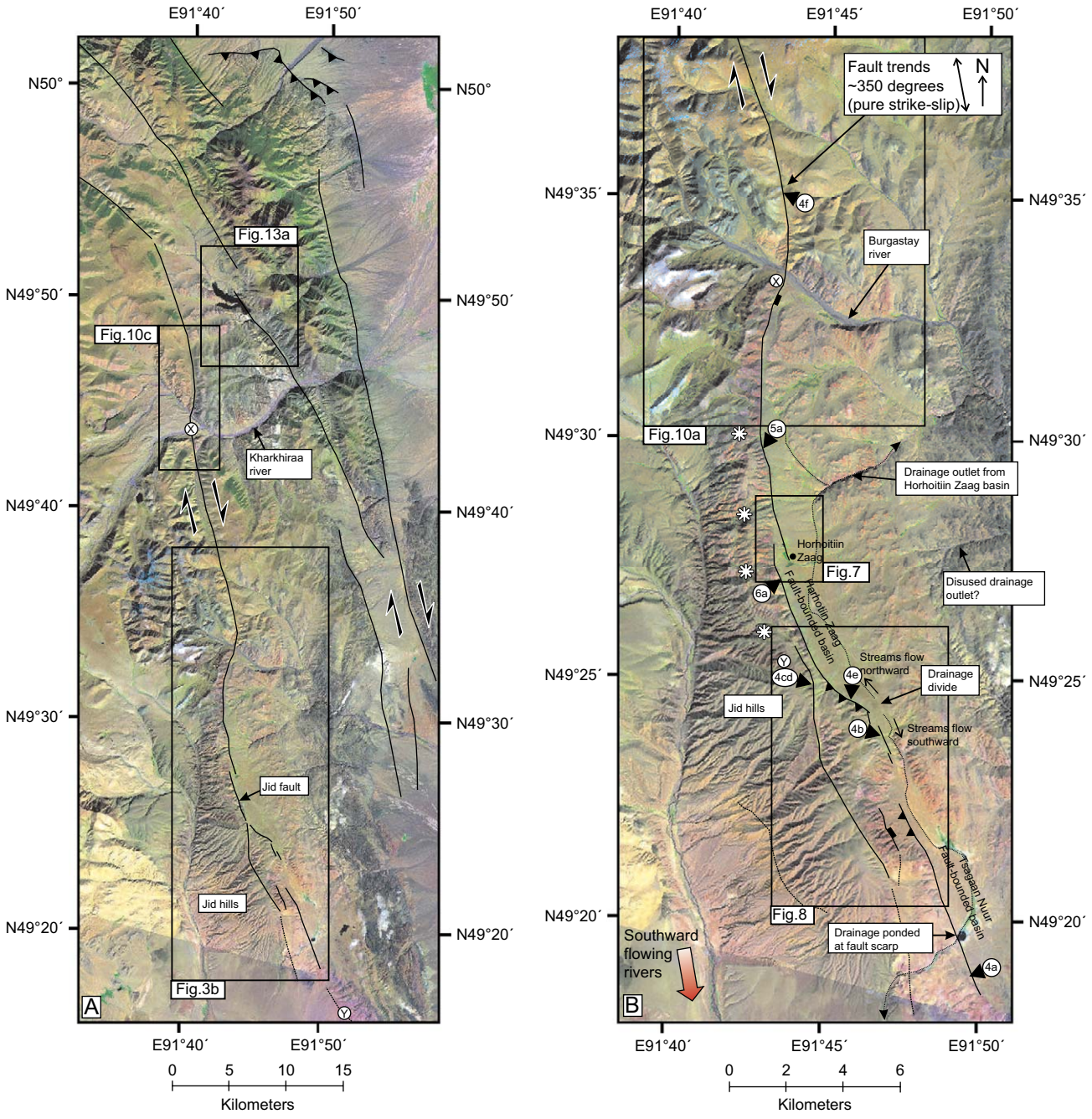

Fig. 3. (A) LANDSAT TM mosaic of the Tsagaan Shuvuut fault zone (see Fig. 2 for location). The mosaic is composed of Landsat scenes 141–25 (2002.08.08), 141–26 (2002.08.08), 142–45 (2000.09.10), 142–26 (2002.07.14) obtained from the Global Land Cover Facility at the University of Maryland (http://glcf.umiacs.umd.edu/index.shtml). In the online colour pdf all Landsat images are displayed as RGB-741. (B) LANDSAT TM mosaic of the Jid fault strand. In the northern part of the image, the fault trends ~350° and has generated very little topography. Bending of the fault south of the Burgastay river is likely to introduce components of extension and convergence. The white stars show the locations of low points in the drainage divide of the Jid hills.

the seismogenic upper crust of 15 km (which is typical of Mongolian earthquakes; e.g. Bayasgalan et al., 2005). Using the relationship $M_w = 2/3 \log M_0 - 6.1$ (Hanks and Kanamori, 1979), our estimate of moment yields a moment magnitude (M_w) of ~7.4. Incidentally, our minimum measured right-lateral displacement of 3.2 m also yields an M_w of 7.5 following the empirical relationship between average surface slip and magnitude described by Wells and Coppersmith (1994).

3.2. Composite scarps and fault structure

Along the northern ~30 km of the part of the Jid fault studied in the field, there are few indications of vertical movements. For example, in Fig. 4F, the fault is expressed as a series of *en echelon* tension fractures, presumably generated during the last slip event, which track across the topography. There is no change in height across these preserved earthquake ruptures, nor is there any evidence of long-term vertical

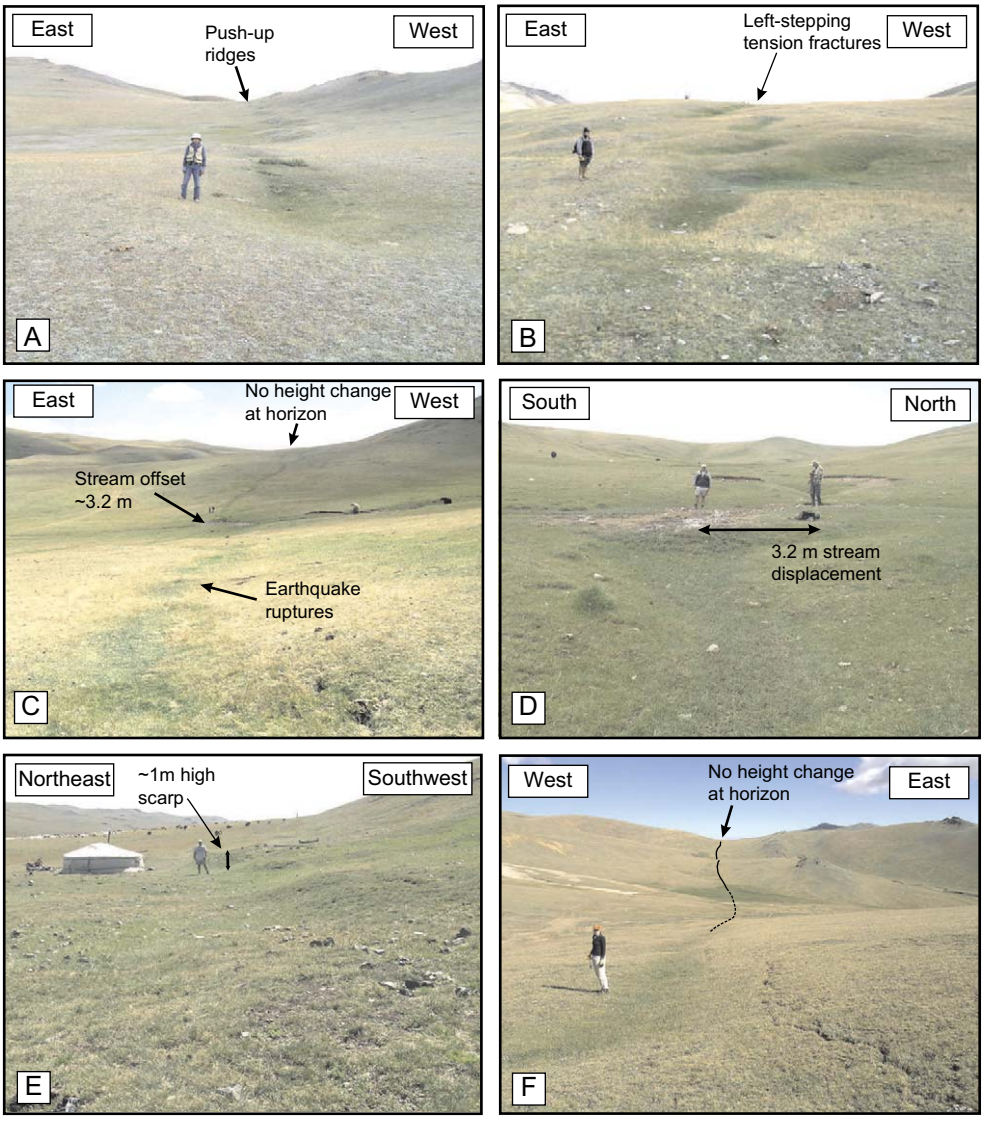

Fig. 4. Photos of earthquake ruptures (arranged from south to north). (A) Right-stepping push-up ridges at 49°18′51.0N, 91°49′48.3E. (B) Left-stepping tension cracks at 49°23′44.3N, 91°46′52.0E. (C) Looking southward along single continuous earthquake rupture at 49°24′57.8N, 91°44′41.6E. (D) Stream displaced by the fault by 3.2 m right-laterally, and ~20 cm vertically (up to the west) at 49°24′54.6N, 91°44′42.5E. (E) Vertical scarp ~1 m high at 49°24′34.0N, 91°45′51.5E. (F) Looking north along the earthquake ruptures at 49°35′01.5N, 91°43′24.9E. There is no change in topography across the fault, and it is likely that the motion here is almost pure strike-slip.

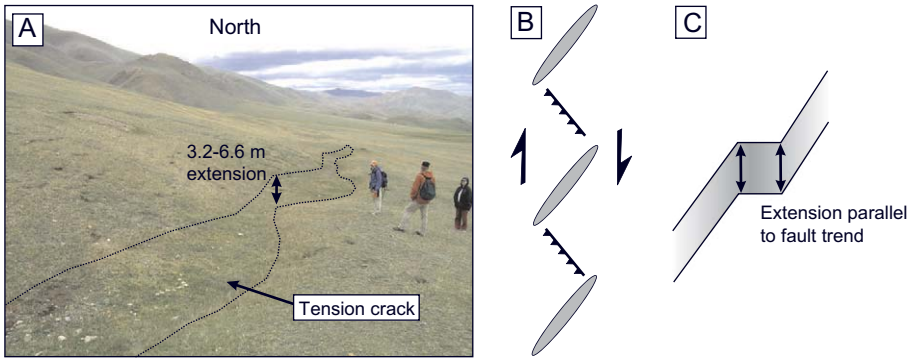

Fig. 5. (A) Photograph looking north of long (~20 m) tension crack at 49°29′45.7N, 91°42′59.1E. The fault continues northward along the base of the Jid hills to the left of the image. The amount of extension measured parallel to the fault trend is 3.2–6.6 m. (B) Sketch of typical strike-slip surface ruptures. Movement on a shear surface at depth is accommodated as a series of tension cracks and push-up ridges oriented at an angle to the overall fault trend. (C) Sketch of the tension fracture seen in (A). The total amount of extension across the crack is measured by correlating between sharp corners in the trace of the crack.

movements in the topography (e.g. Fig. 4F). In this region, the fault strikes at ~350°, and we are therefore confident that the regional slip-vector is also ~350°. This value is in agreement with slip-vectors determined from the modelling of recent earthquakes in other parts of the Altay (Bayasgalan et al., 2005).

South of the Burgastay river, the Jid fault shows substantial vertical displacements within Quaternary deposits (e.g. Fig. 6). Where the overall strike-slip direction of 350° differs from the local trend of the fault, a component of dip-slip movement should result, with a normal component expected between latitude 49°34′N and 49°28′N, and an overall reverse component further south.

3.2.1. Dip-slip faulting in the Horhoitiin Zaag basin

The apparent vertical displacement across the fault along the Horhoitiin Zaag basin is often greater than the real vertical displacement (e.g. Fig. 6). Closely spaced streams flow eastward from the Jid hills into the basin. Each stream has deposited a small gravel fan along the eastern margin of the hills, resulting in a gently undulating topography (e.g. Fig. 6A). The Jid fault cuts through each fan close to its apex (e.g. Fig. 6B). If the fault has a small dip-slip component of motion (distance *B* in Fig. 6C), the lateral displacement of topography across each fan will generate large apparent vertical offsets across one margin of the fan (distance *A* in Fig. 6C), and much smaller vertical offsets at the other edge of the fan (e.g. Regard et al., 2005). The right-lateral motion across the fan in Fig. 6A is ~10–15 m, which is similar to values measured across many other displaced alluvial fans along the fault (see Section 3.3.2).

Everywhere south of the Burgastay river the western side of the fault is uplifted. If the dip-slip component of motion is introduced by bending along the trace, the dip of the fault must change southward from an eastward dip (with a normal component) to a westward dip (with a reverse component). The change from normal to reverse faulting inferred from the fault orientation coincides with a segment boundary and small pull-apart basin at Horhoitiin Zaag village (Fig. 7). As the Jid hills are likely to result from dip slip on the fault (see Section 3.3.1) the height of the hills should decrease substantially where the dip of the fault changes from east to west. However, the Jid hills do not reduce in height adjacent to Horhoitiin Zaag village, and it is possible that the change in fault dip occurs at the southern margin of the basin at ~49°25′N, where the fault begins to show a very clear reverse component (see Section 3.2.2).

The geomorphology of the Horhoitiin Zaag pull-apart basin indicates an evolution of faulting (Fig. 7), with the eastern fault strand apparently increasing its length to the south over time. Streams flowing eastward from the Jid hills are ponded against the newly formed eastern scarp, forming marshy ground, and resulting in the southward deflection of streams around the end of the scarp (Fig. 7C). An earlier, abandoned, stream channel is preserved as a linear grassy depression visible in the aerial photographs (Fig. 7A). As the northern segment grows in length, the southern segment appears to be retreating southward, and the fresh scarps observed along the base of the Jid hills become progressively more eroded and eventually disappear in the overlap zone between the two segments (Fig. 7).

3.2.2. Shortening south of the Horhoitiin Zaag basin

Between latitude 49°25′N and the southern end of the fault the Jid fault splits into several sub-parallel strands (Fig. 8). Holocene scarps and earthquake ruptures are observed along the faults marked in Fig. 8A and all seem to be active at the present-day. The fault has an overall strike of ~340°, and should have a slight component of shortening given the ~350° regional slip-vector azimuth inferred earlier (see Section 3.2). In the northern part of Fig. 8, the fault splits into two strands. The western strand (labelled A in Fig. 8A) has a relatively linear trace as it cuts across undulating topography and appears to displace streams and interfluves right-laterally, from which we infer a steep-dipping right-lateral strike-slip fault. We followed fault strand A southward to 49°24′N. Clear

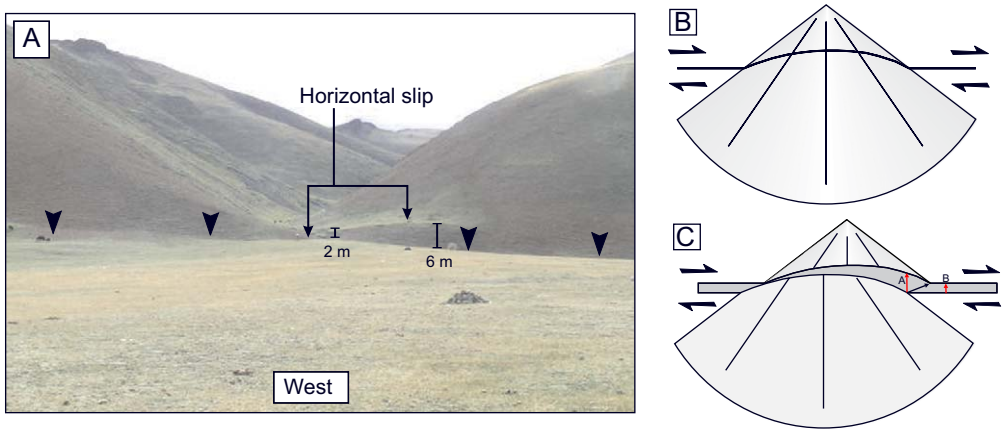

Fig. 6. (A) Composite scarp viewed looking west from 49°27′05.5N, 91°43′42.6E. The scarp has a height of ~6 m. The real vertical displacement is ~2 m, with a right-lateral displacement of ~10–15 m. (B) Sketch of an alluvial fan deposited across the trace of the fault. (C) Sketch of the effect of strike-slip displacement on producing large apparent vertical offsets (adapted from Regard et al., 2005). The lateral displacement of topography at the margin of the fan produces vertical scarps with apparent heights (*A*) which are much larger than the true vertical displacement (*B*).

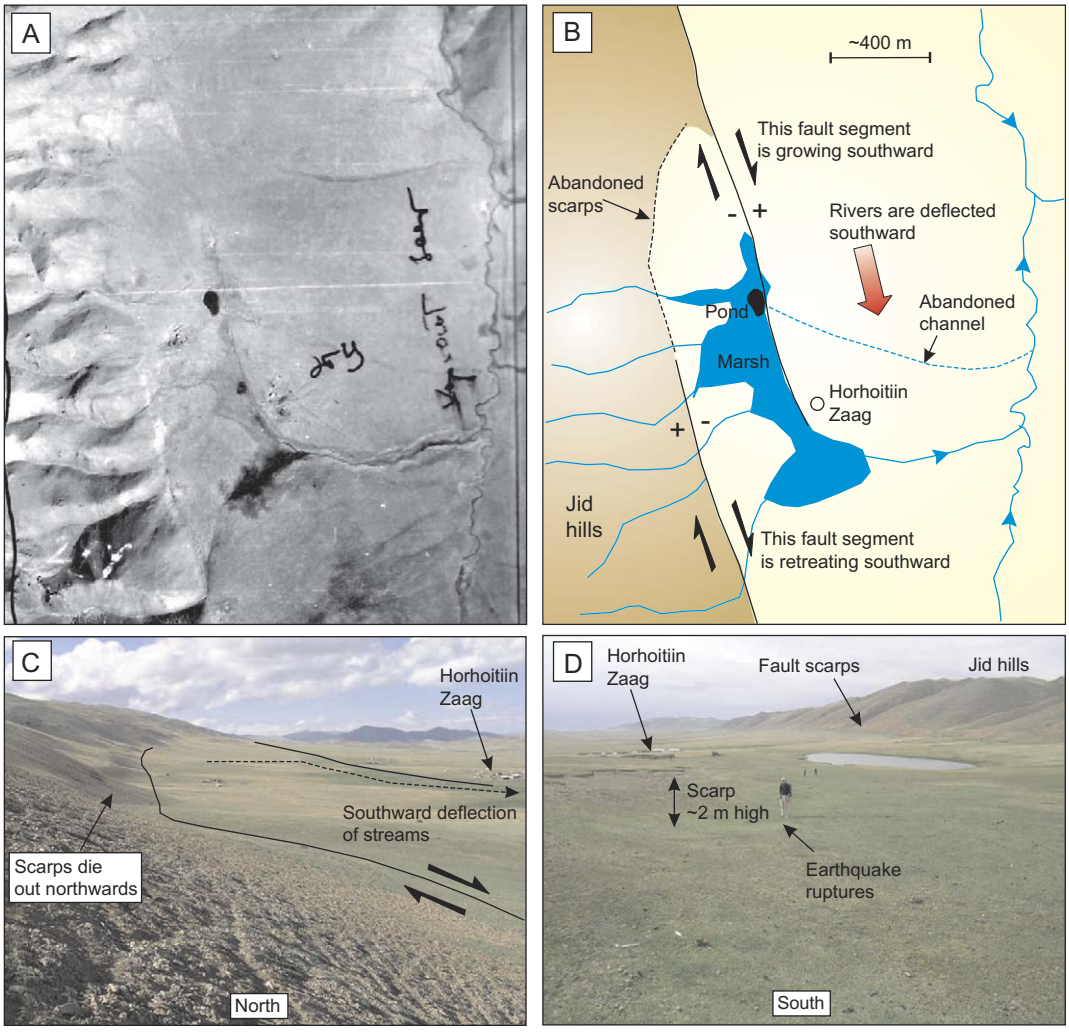

Fig. 7. (A) Aerial photo of segment boundary and pull-apart basin at Horhoitiin Zaag village. See Fig. 3B for location. (B) Interpretive map of the view in Fig. 6A. The northern segment appears to be actively growing southward at the expense of the southern segment, which becomes progressively more eroded northward. The southward growth of the northern segment has caused ponding and southward deflection of eastward-flowing drainage. Evidence of an older drainage channel is preserved as a dry valley. (C) View northward from 49°26′59.3N, 91°43′34.0E of the Horhoitiin Zaag pull-apart. (D) View southward from 49°27′53.8N, 91°43′36.5E of the scarp of the northern segment with fresh earthquake ruptures.

earthquake ruptures were identified along the fault with displacement of 3.2 m right-lateral and ~20 cm vertical, up to the west (Fig. 4C,D). We saw no large cumulative vertical scarps along the line of strand A, which follows a wide valley with subdued relief (Fig. 4C), and it is therefore likely that the motion on this fault strand is predominantly strike-slip.

In contrast, the eastern fault strand (B) shows abundant evidence of uplift across the fault. A continuous scarp, ~1 m high, was found along the base of a steep cumulative scarp (Fig. 4E). This section of the fault trends at ~305°, and so a large component of shortening would be expected. Partially infilled tension cracks were found along the top of the scarp, which presumably show extension and collapse of the scarp, as observed in the co-seismic ruptures of many recent thrust earthquakes, such as the 1980 El Asnam earthquake in Algeria (e.g. Yielding et al., 1981; Philip and Megraoui, 1983), and the 1988 Spitak earthquake in Armenia (e.g. Philip et al., 1992). The tension cracks are arranged *en echelon* and indicate a component of right-lateral shear (e.g. Bayasgalan et al., 1999a).

The large component of shortening across fault strand B coincides with a topographic and drainage divide for streams flowing axially along the Horhoitiin Zaag and Tsagaan Nuur basins (Figs. 8 and 9). It seems reasonable that the local increase in elevation east of the fault, and therefore the evolution of the drainage systems within the basins, are controlled by the locally enhanced uplift across the Jid fault. Close to the drainage divide, the faults appear to have migrated eastward from the range-front, and earthquake ruptures follow a pair of low linear ridges which deflect drainage flowing eastward from the Jid hills (Fig. 9). Wind-gaps in the ridges show the original eastward course of the streams (Fig. 9B,C).

For ~3 km south of latitude 49°23′N, three sub-parallel active fault strands are present within a zone only ~2 km wide. As described earlier, we interpret strand A as a steeply dipping strike-slip fault. In contrast, strand C has a considerable dip-slip component with east-facing scarps developed in alluvial fans (Fig. 8). From the way it tracks across the undulating topography, strand C appears to dip eastward, and

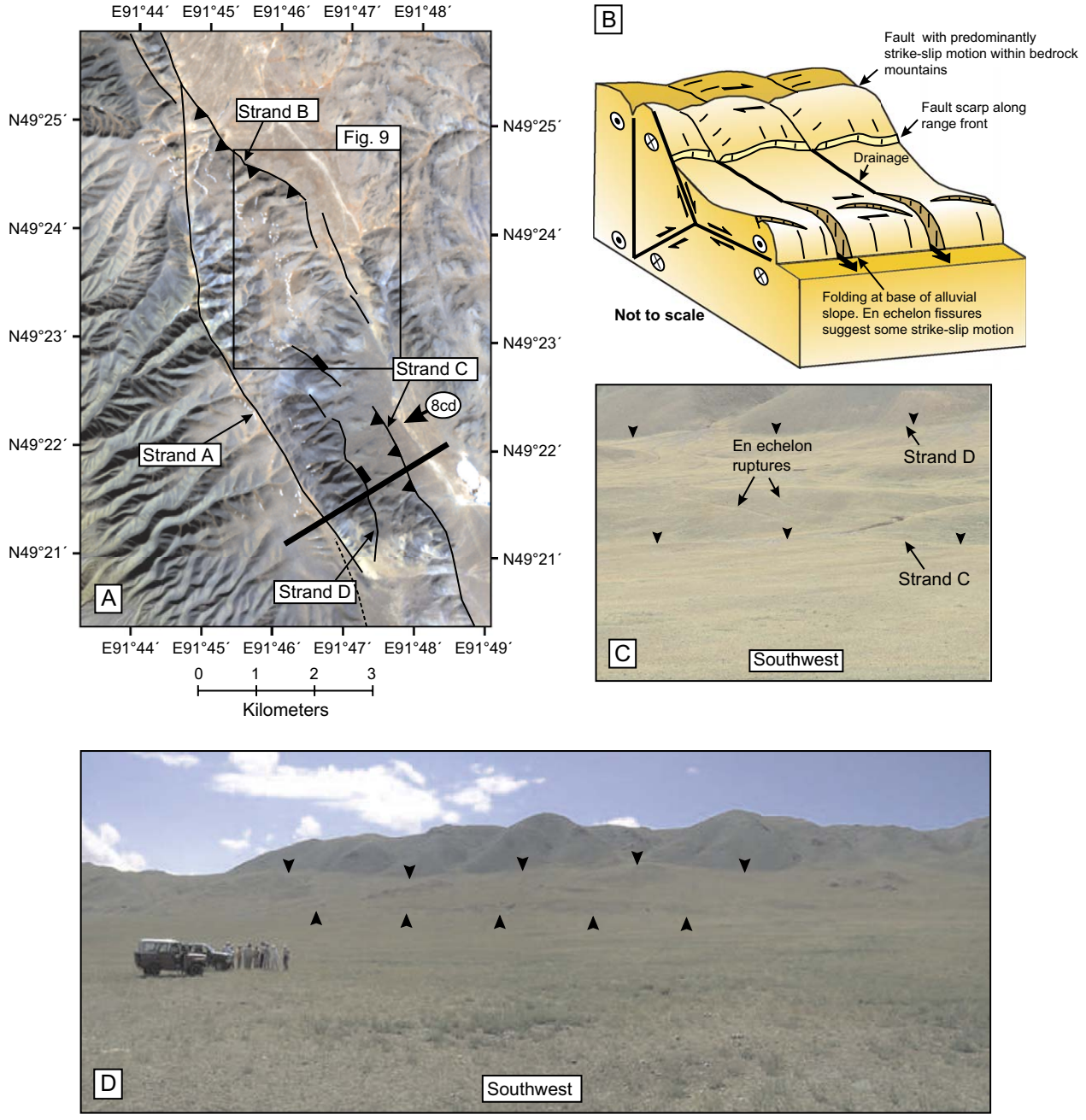

Fig. 8. (A) ASTER satellite image of parallel fault strands (labelled A–D) and flower structure at the southern margin of the Horhoitiin Zaag basin. The ASTER image dates from 2001.03.30 and is displayed as RGB-321 in the online colour version. See Fig. 3B for location. (B) Sketch of possible fault structure at depth, along the line of section (thick black line) in (A). (C) View westward from 49°22′11.5N, 91°47′49.7E at the anticlinal ridge with left-stepping tension cracks along its axis. Fault strand C, with a probable normal component, can be seen in the distance. (D) View from 49°22′10.6N, 91°48′06.3E looking west across fault strands C and D.

therefore has a normal component. Strand D, however, is developed as a low anticlinal fold within alluvial deposits shed from the Jid hills to the west. Partially infilled left-stepping *en echelon* tension fractures run along the axis of the fold (e.g. Fig. 8C). The tension fractures show that the fold accommodates components of both shortening and right-lateral strike-slip.

The sub-parallel fault strands with strike-slip, normal and oblique thrust components are likely to be underlain by a single oblique slip fault at depth (e.g. Fig. 8B). We have no constraints on the faulting beneath the point where the three surface strands join, and so we do not attempt to interpret the deep structure in Fig. 8B. Such structures are often called flower structures from their appearance in cross-section. The widening of the Jid fault zone may be influenced by the right-step between fault strand A, which appears to die out to the south, and strand D which continues across the Tsagaan Nuur basin to the southern end of the Jid fault and shows abundant signs of recent activity, with well-preserved earthquake ruptures (Fig. 4A), and ponding of drainage across a low

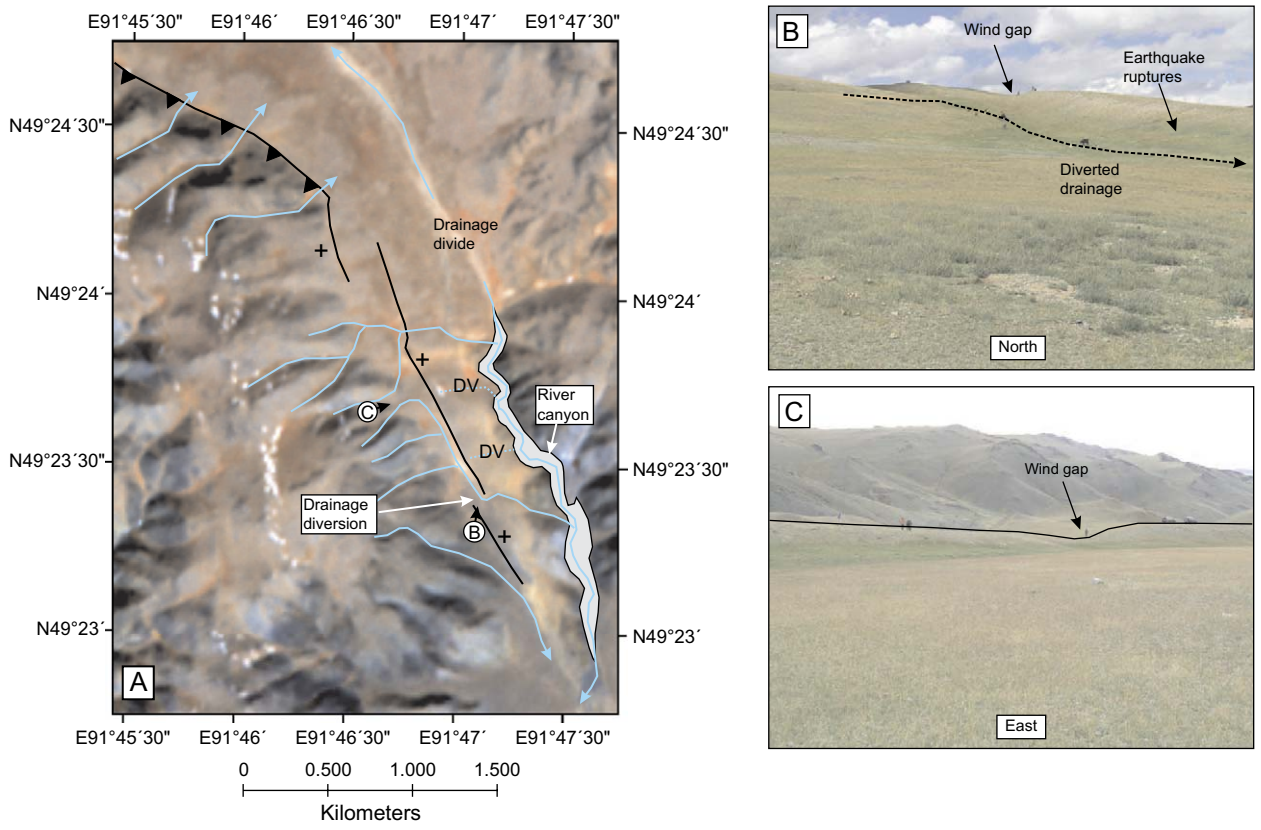

Fig. 9. (A) ASTER satellite image (see Fig. 8 for location) of faulting at the divide between streams flowing northward into the Horhoitiin Zaag fault-bounded basin, and drainage flowing southward into the Tsagaan Nuur fault-bounded basin. Eastward-flowing streams are deflected southward around the ends of short (0.5–1 km in length) *en echelon* fault segments. Older stream courses are preserved as dry valleys (labelled DV), which show as wind-gaps in the ridges. (B) View north from 49°23′26.9N, 91°47′02.7E of fault ridge with wind-gap and southward deflected streams. (C) View east from 49°23′34.4N, 91°47′01.1E of wind-gap in cumulative fault scarp. The black line outlines the top of the small ridge.

east-facing scarp (Fig. 3B). The enhanced component of shortening in the overlap zone between strands A and D may have led to the development of a flower structure.

3.3. Total slip and averaged slip-rate on the Jid fault

3.3.1. Total slip estimates

Close to the Burgastay river (Figs. 3B and 10), the Jid fault bends to the right, enhancing the normal component of motion, and opening a narrow pull-apart basin. The basin has been filled by sediments deposited by closely spaced streams flowing east from the Jid hills. In Fig. 10B, we have restored 1 km of right-lateral slip on the Jid fault, assuming that pure strike-slip motion has a slip-vector azimuth of ~350° (see Section 3.2). Restoration of 1 km of slip re-aligns a series of eastward-flowing rivers, including the Burgastay river, and closes the narrow pull-apart basin. It is very likely that the 1 km of slip represents the total slip of this part of the fault. Restoration of ~1 km of right-lateral slip also closes another narrow fault-bounded pull-apart basin at the northern bank of the Kharkhiraa river (Fig. 10C).

The total amount of vertical displacement varies along the fault. In the area north of the Burgastay river no vertical displacement is seen across the preserved earthquake ruptures (Fig. 4F), and there is no significant change in elevation of the mountains on either side of the fault. Further south, a vertical component of slip is introduced where the fault bends around the side of the Horhoitiin Zaag basin (Fig. 3B), with oblique fault movement forming the Jid hills. Profiles drawn through the SRTM digital topography data set show an average of ~300 m elevation change between the crest of the Jid hills and adjacent parts of the basin (e.g. Fig. 11B).

The ~300 m of elevation change between the Jid hills and the Horhoitiin Zaag basin is reasonable given that the total horizontal displacement on the fault is ~1 km, and that the vertical displacement is introduced by bends in strike of ~10–20°. It is therefore probable that the Jid hills did not exist before the fault was initiated. At the present-day, rivers flowing eastwards from the Kharkhiraa massif bend abruptly southward at the Jid hills (e.g. Fig. 3). A north–south topographic profile along the crest of the Jid hills (Fig. 11A) shows several low points which align with linear east–west valleys through the hills (marked by white stars in Fig. 3B). To the eastern side of the fault-bounded basins, there are numerous apparently abandoned drainage channels, with almost all drainage in the northern Horhoitiin Zaag fault-bounded basin presently draining eastward through one outlet, and all drainage in the southern Tsagaan Nuur basin draining westward through a single outlet at the southern end of the fault (Fig. 3B). These observations suggest that the uplift of the

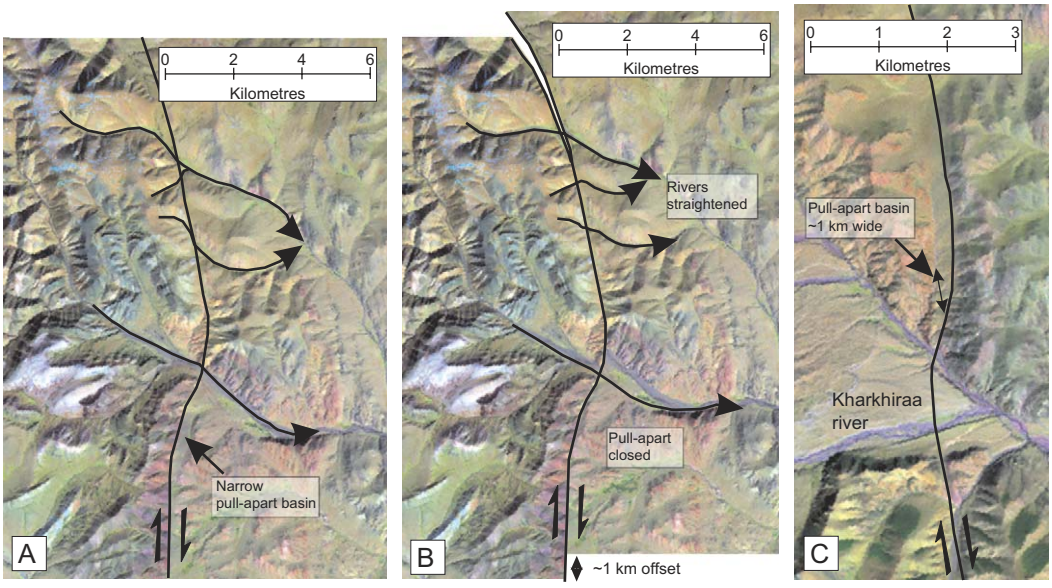

Fig. 10. (A) LANDSAT image of the Jid fault in the region of the Burgastay river. See Fig. 3B for location. (B) The same image, but with 1 km of right-lateral slip restored. The four eastward-flowing rivers have been restored to linear courses, and the narrow pull-apart basin at the southern end of the image has been closed. (C) LANDSAT image of a small pull-apart basin north of the Kharkhiraa river (see Fig. 3A for location). Restoration of ~1 km of slip closes the basin.

Jid hills has blocked an originally eastward-flowing drainage network and diverted the active channels southward. The low points in the topographic divide of the Jid hills might represent the remnants of the original eastward-flowing drainage courses, though this interpretative is speculative. If our interpretation is correct, the Kharkhiraa mountains are older than the Jid fault. We explore the implications of this further in the discussion.

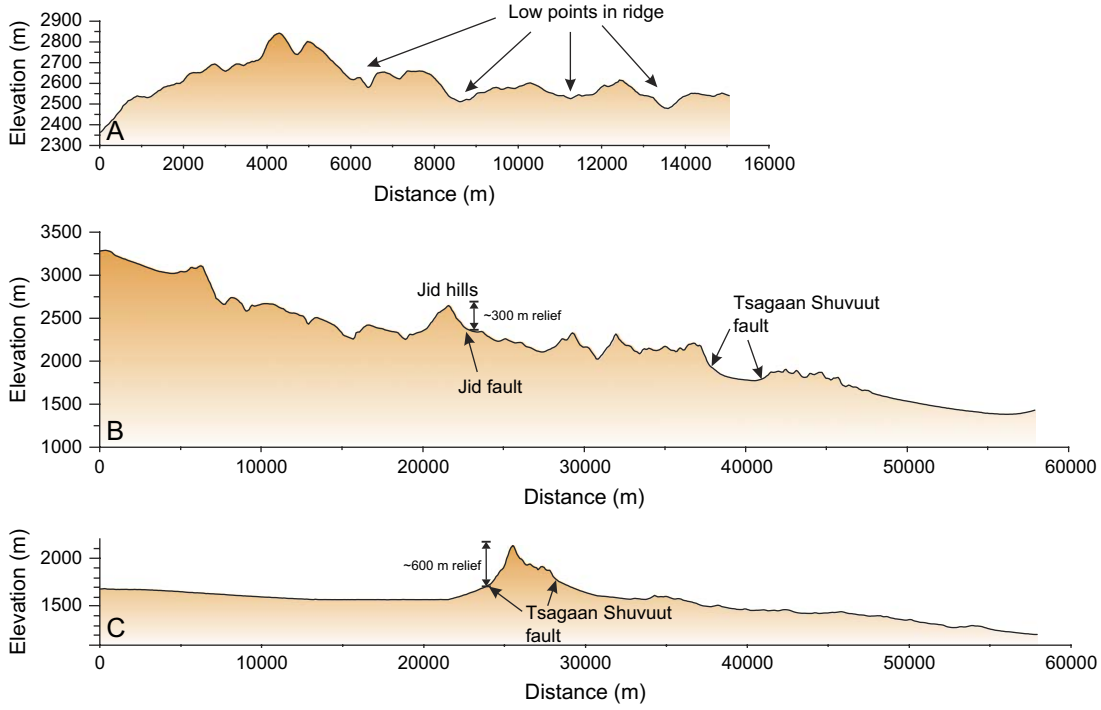

Fig. 11. Profiles through SRTM digital topography. (A) North–south profile along the drainage divide of the Jid hills. The end points of the profile are marked X and Y in Fig. 3B. Low points in the ridge may represent the remains of older drainage channels which have now been diverted by uplift of the Jid hills. Alternatively, they may represent erosional features post-dating uplift of the ridge. The positions of the low points are marked as white stars in Fig. 3B. (B) Regional east–west profile from the Kharkhiraa mountains to the Uvs Nuur basin at longitude ~49°30′N. Height changes across the Jid fault, and other strands of the Tsagaan Shuvuut fault system, are minor when compared to the overall regional topographic slope. Line of profile is marked in Fig. 2. (C) Regional east–west profile at longitude ~49°N. The height change across the fault is only ~600 m.

3.3.2. Slip-rate estimates

The youngest generation of alluvial fan surfaces within the pull-apart basin south of the Burgastay river is abandoned, and eastward-flowing streams now exit the mountains through narrow channels cut into the fans (Fig. 12A,B). The top surface of each fan has been offset across the fault, leaving a vertical scarp ~5 m high (Fig. 12B), and also an apparent right-lateral displacement of ~10–15 m. The estimates of displacement were measured in the field by eye and are likely to involve several metres of uncertainty. In particular, the horizontal displacements are difficult to determine with certainty as the edges of the fans are diffuse. A stream incised into the most recent fan deposits at 49°31′39.1N, 91°42′53.6E, is also displaced by ~9 m across the fault. The vertical displacements

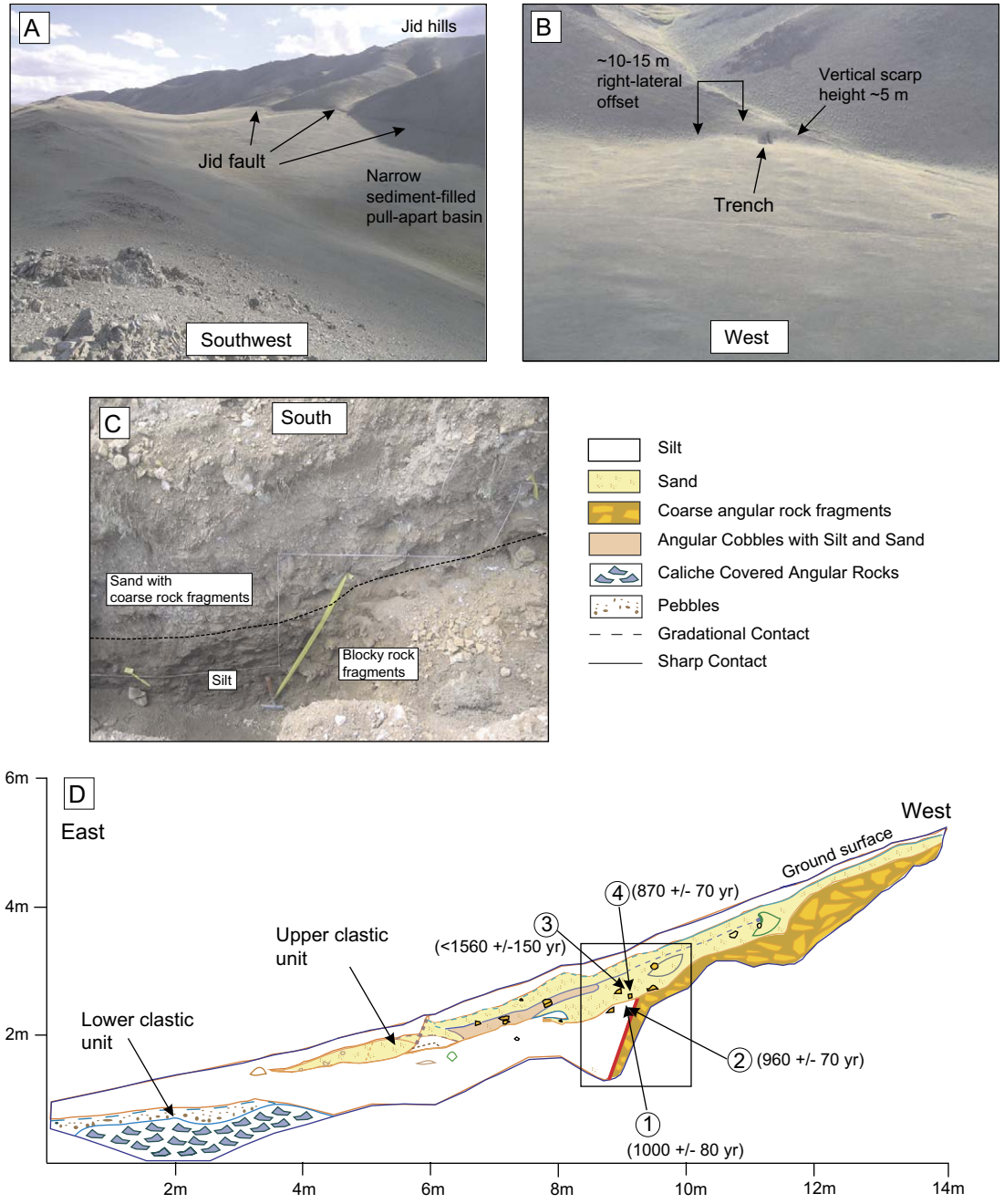

Fig. 12. (A) View SW from 49°32′25.4N, 91°43′23.7E across the narrow pull-apart basin south of the Burgastay river. Cumulative fault scarps run along the base of the Jid hills at the western side of the basin. (B) View westward from 49°32′27.2N, 91°43′21.0E at a small alluvial fan cut by faulting, through which a trench has been excavated. The cumulative eastward-facing scarp is ~5 m high. The margin of the fan is displaced by ~10–15 m right-laterally (based on field observations, difficult to see in photograph). (C) Photo of the Jid fault exposed in the southern wall of the trench in Fig. 11D. The fault is marked by yellow tape. (D) Interpretation of sediments and structures exposed in the southern wall of a trench through the fault at 49°32′43.2N, 91°43′06.6E. An upper clastic unit postdates the most recent visible faulting. Two OSL samples (1 and 2) are taken from the uppermost part of the silt exposed on the downthrown side of the fault. The other two OSL samples (3 and 4) are from the base of the clastic unit, which is not cut by faulting. The OSL samples thus bracket the date of the last fault movement at ~870–980 years ago. The box shows the approximate area visible in Fig. 11C.

may be underestimated due to on-going sedimentation on the downthrown side of the fault (as seen in a trenched section through the fault, see Section 4). The vertical displacement of the fan surfaces appears to decrease southward, as the fault acquires more of a strike-slip component in the Horhoitiin Zaag basin (e.g. Fig. 6).

The similarity of the measured displacement across each fan suggests that they were all abandoned at roughly the same time, and may reflect a regional change in the hydrology of the rivers. Cycles of deposition and subsequent abandonment of alluvial fans on a regional scale are often correlated to climatic changes (e.g. Ritz et al., 1995; Pan et al., 2003), with the most recent period of widespread fan deposition occurring after the last glacial maximum, when the onset of a warmer and more humid climate would have mobilised sediment that had been stored in mountainous regions during the cold and arid glacial period (e.g. Poisson and Avouac, 2004). Exposure dating of fan surfaces in the Gobi–Altay of southern Mongolia suggests an age of ~20 ka for abandonment of the most recent alluvial fans (e.g. Ritz et al., 1995; Vassallo et al., 2005). We did not find dateable material to confirm the age of abandonment of the fans. However, the onset of post-glacial conditions in western Mongolia is thought to have occurred roughly 10–15 ka ago (e.g. Lehmkuhl, 1998; Grunert et al., 2000). Similar ages for post-glacial warming are found in surrounding regions such as the Gobi desert (e.g. Owen et al., 1998). If we assume that the fans along the Jid fault were abandoned at 10–15 ka, the ~10–15 m of right-lateral displacement across the fans indicates a slip-rate of ~1 mm/yr. However, given the likely uncertainties of several metres in our measurements of the lateral offset of the fans, even if the fans along the Jid fault were abandoned at ~20 ka, as suggested by the results of exposure dating in southern Mongolia (e.g. Vassallo et al., 2005), it does not make significant difference to our estimate of slip-rate.

The total cumulative displacement of 1 km determined in the previous section would accumulate in ~1 Ma at a rate of 1 mm/yr. This value suggests the Jid fault is relatively young in comparison to the Miocene onset of uplift in the Mongolian Altay (see Section 2).

4. Dating the last earthquake on the Jid fault

A 14.5-m-long trench was dug across the Jid fault at 49°32′43.2N, 91°43′06.6E, where it cuts one of the small alluvial fans described in the previous section (Fig. 12). The 10–15 m of right-lateral displacement measured across the fans indicates that several slip events have occurred since deposition of the fan material. Rather than providing a complete history of recent earthquakes on the Jid fault, our aim in digging the trench was simply to date the most recent slip event, in order to provide constraints on the age of the earthquake ruptures described in Section 3.1. In the following paragraphs, we describe the southern wall of the trench, from which we took samples for dating. The northern wall shows the same relationships.

The trench revealed a normal fault dipping ~70° to the east, which separates coarse quartzite rock debris on the upthrown side, from accumulations of dark silt (loess), with two units of coarser material (colluvium), on the downthrown side (Fig. 12C,D). The quartzite rock debris has a matrix of orange sand and clay. The silt exposed on the downthrown side of the fault is dark brown in colour with occasional laminations.

The fault, and the deposits separated across the fault, is covered by an unbroken, wedge-shaped, and eastward-thinning layer of orange-coloured rock debris (marked as clastic unit 1 in Fig. 12D). We interpret this unit as a colluvial wedge corresponding to the degradation of a scarp. There are no indications anywhere along the trench wall that the wedge is cut, or in any way deformed, by faulting. We are therefore confident that deposition of the wedge of coarse material postdates the most recent movement on the fault. The wedge is in turn covered by a ~50 cm thick layer of silt which again shows no evidence of deformation. A second clastic unit is exposed at the lowest part of the trench exposure (Fig. 12D). This unit is potentially a colluvial wedge associated with an earlier earthquake event. Apart from the two colluvial wedge units, the downthrown side of the fault exposes uniformly fine-grained silt.

The deposition of the wedge of coarse-grained sediments must therefore postdate the last slip event, and the age of deposition will thus provide a minimum age constraint on the most recent earthquake. The silt deposits exposed on the downthrown side of the fault should pre-date the last fault movement. We took four sediment samples of the silt (loess) for OSL dating to bracket the last fault movement (see Fig. 12D and Table 1). Brief details of the analytical procedures are given in the legend for Table 1. Two samples of silt-sized sediment from the base of the upper clastic layer gave ages of 870 ± 70 years (sample 4) and $<1560 \pm 150$ years (sample 3). Two samples from silts just below the base of the upper clastic unit gave ages of 1000 ± 80 years (sample 1) and 960 ± 70 years (sample 2). A minimum age of 870 ± 70 years is therefore found for the last movement on the fault. OSL samples 1 and 2 from the lower silt unit provide maximum age constraints of 1000 ± 80 years and 960 ± 70 years. Taking an average of the two values yields an age of ~980 years.

As discussed in Section 3.1, surface ruptures are observed for at least 55 km along the fault, and from the measured displacements across them, are likely to have been generated during a single earthquake of M_w ~7.5 which ruptured the entire ~90 km length of the Jid fault. From the OSL dates presented above it appears that the last large earthquake occurred between ~870 years and 980 years ago. This date for the Jid earthquake is compatible with the level of preservation of the ruptures when compared qualitatively with other preserved surface ruptures in Mongolia (e.g. Baljinnyam et al., 1993).

5. Constraints on the evolution of the Tsagaan Shuvuut fault zone

In the previous sections, we have used observations of the landscape to unravel aspects of the structure, the evolution

Table 1
Optically stimulated luminescence (OSL) ages and associated chronological data for loess sediments collected from a trench at 49°32′43.2N, 91°43′06.6E (see Fig. 11)

Field no.	Lab no.	Equivalent dose (Grays)	*A* value	Uranium (ppm)	Thorium (ppm)	K_2O (%)	Moisture content	Total dose rate (Grays/ka)	OSL age
LS1	UIC1531	3.070 ± 0.050	0.082 ± 0.003	1.69 ± 0.25	4.73 ± 0.67	1.75 ± 0.02	10 ± 3	3.08 ± 0.14	1000 ± 80
LS2	UIC1532	2.916 ± 0.032	0.050 ± 0.001	1.72 ± 0.31	5.98 ± 0.86	1.76 ± 0.02	10 ± 3	3.03 ± 0.14	960 ± 70
LS3	UIC1533	$<4.151 \pm 0.276$	0.042 ± 0.001	1.70 ± 0.25	4.83 ± 0.63	1.42 ± 0.01	10 ± 3	2.65 ± 0.13	$<1560 \pm 150$
LS4	UIC1534	2.363 ± 0.060	0.055 ± 0.003	1.79 ± 0.24	4.17 ± 0.62	1.56 ± 0.02	10 ± 3	2.73 ± 0.13	870 ± 70

The equivalent dose is determined under infrared stimulation (880 ± 80 nm) on the fine-grained (4–11 μm) polymineral extract for all samples. The multiple aliquot additive dose method (e.g. Forman and Pierson, 2002) is used. Blue emissions are measured with three 1-mm-thick Schott BG-39 and one 3-mm-thick Corning 7–59 glass filters that block >90% luminescence emitted below 390 nm and above 490 nm in front of the photomultiplier tube. The measured alpha efficiency factor (*A* value) is as defined by Aitken and Bowman (1975). U and Th values are calculated from the alpha count rate, assuming secular equilibrium. K_2O values are determined by ICP-MS (Activation Laboratory Ltd., Ontario). The total dose rate contains a cosmic ray dose rate component of 0.28 ± 0.03 (Prescott and Hutton, 1994). All errors are at one sigma. Analyses were performed by the Luminescence Dating Research Laboratory, Department of Earth and Environmental Sciences, University of Illinois – Chicago.

through time and also the behaviour of the Jid fault in individual earthquake events. We now use remote sensing imagery to briefly describe the development of the Tsagaan Shuvuut fault zone as a whole, and to investigate the role of the Jid fault in the generation of topography in adjacent parts of the Mongolian Altay mountains.

The Kharkhiraa and Türgen Uul massifs are situated along the western margin of the Tsagaan Shuvuut fault zone, and on initial inspection, might be considered to be caused by uplift across the Tsagaan Shuvuut fault. However, as we saw in Section 3.3.1, the total vertical displacement on the Jid fault, which is the closest of the Tsagaan Shuvuut strands to the high mountains, is likely to be only ~300 m. Even this 300 m of vertical displacement is not evenly distributed along the fault and is instead introduced by departures in the strike of the fault from the 350° direction of 'pure strike-slip' determined in Section 3.2. Also in Section 3.1, we saw that the Jid fault has apparently disturbed an older and eastward-flowing drainage network which originated in the Kharkhiraa mountain. Movement on the Jid fault is therefore likely to postdate the initiation of uplift of the high mountainous areas.

Slip on the Jid fault is therefore neither sufficiently large, nor sufficiently old, to account for the adjacent topography in the Kharkhiraa and Türgen Uul massifs. Indeed, there is no real indication in the regional geomorphology that the Tsagaan Shuvuut fault zone as a whole shows any substantial

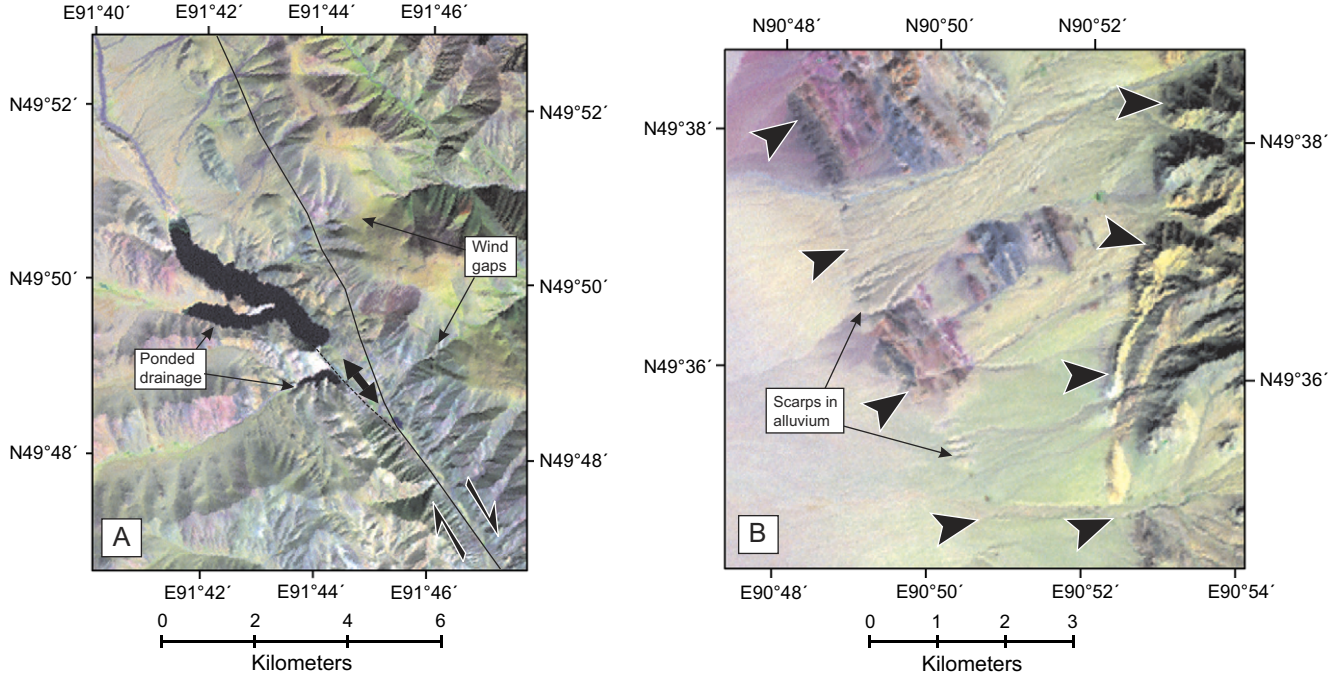

Fig. 13. LANDSAT TM images of faulting to the east and west of the Jid strand. (A) Image showing right-lateral stream offsets of ~1 km on the central strand of the Tsagaan Shuvuut fault (see Fig. 3A for location). Localised uplift of the eastern side of the fault has dammed the eastward-flowing drainage, which has now ponded in small lakes. The original outlets are preserved as wind-gaps in the ridge of mountains east of the fault. (B) Eastward-dipping thrust faults bounding the edge of the Achit Nuur depression (see Fig. 2 for location). Black arrows point to the scarps. The eastern scarp separates bedrock exposure (to the east) from alluvium. The western scarp is in alluvial fan material and forms a prominent west-facing step in the sediment.

vertical component of motion, apart from where its orientation departs from 350°. In the southern part of Fig. 2, for example, the Tsagaan Shuvuut fault strikes at ~350°, and cuts across a relatively flat plain of low elevation (see Fig. 11C), but produces a maximum of only ~600 m of relief. Even this relatively small amount of relief is localised at small changes in fault orientation. It is only when the fault starts to bend significantly at latitude ~49°15′N that elevation changes start to appear across the fault, as for example in Fig. 13A, where uplift between the eastern and central Tsagaan Shuvuut strands is localised to a region close to Ulaangom city where the faults bend to the left (e.g. Fig. 2). Note that as well as showing dip-slip movement, the streams in Fig. 13A are also displaced right-laterally by ~1 km, giving a minimum total strike-slip displacement on the central Tsagaan Shuvuut fault strand. Further north on this central strand, another series of small rivers are displaced right-laterally by ~1 km, at ~50°01′N, 91°31′E.

A number of recently active north–south thrust faults can be inferred from satellite imagery along the eastern margin of the Achit Nuur depression (Fig. 13B). These faults appear to be uplifting the western margin of Kharkhiraa and Türgen Uul (e.g. Fig. 2). However, these faults do not account for the elongated WNW–ESE shape of the massifs, and the WNW–ESE oriented drainage divides within them (Fig. 2), which would be expected to be parallel to the direction of the thrusts (e.g. Cunningham et al., 2003). The implication is that the two massifs must have been uplifted on thrusts at their northern and southern margins which are not obvious in the satellite imagery. We have marked inferred faults along the sharp bases of the Kharkhiraa and Türgen Uul mountain ranges in Fig. 2, but without field observations, we are not certain as to whether these sharp breaks in slope are actually faults, and if they are, whether or not they are still active at the present-day.

In summary, the topography of the study region is somewhat puzzling. It appears that the two glaciated massifs were uplifted on predominantly WNW–ESE structures. At present, however, the dominant structures are oriented N–S, with right-lateral strike-slip along the eastern margin of the mountains, and eastward-dipping thrusts on the western margin. The conclusion from this is that the pattern of faulting has changed through time. Potentially this is due to a northward propagation of the termination of the Tsagaan Shuvuut fault system, which ends at present in the east–west Tsagaan Shuvuut Uul range, but which might have originally terminated at east–west thrust faults bounding the Kharkhiraa and Türgen Uul mountain ranges. Lateral growth of strike-slip faults by the propagation of new terminating thrusts has also been suggested for faults in the Gobi–Altay (Bayasgalan et al., 1999b).

6. Conclusions

We conclude that the Jid fault last moved ~900 years ago in an earthquake of M_w ~7.5, and which generated right-lateral slip of ~5 m. The total displacement on the fault is ~1 km. At the inferred Holocene slip-rate of ~1 mm/yr, the fault would have initiated ~1 Ma ago. The Jid fault is one strand of the Tsagaan Shuvuut fault system. The geomorphology suggests that the height of the Kharkhiraa and Türgen Uul mountains cannot be accounted for by oblique slip on the Tsagaan Shuvuut faults and that the massifs must instead have been uplifted on thrust faults propagating westward from the Tsagaan Shuvuut fault system.

Indications of active faulting are very well preserved in Mongolia, presumably due to the cold, and relatively arid climate. It is the pristine geomorphology, and in particular the superb preservation of surface ruptures from an ancient earthquake event, that have allowed us to infer details of fault structure and evolution with applicability to zones of active faulting and earthquake hazard worldwide. The long record of preserved earthquake deformation in Mongolia therefore makes it an ideal region for the study of active faulting from the landscape.

Acknowledgements

We thank the Datsan Trade company for their kindness in the field, for logistical help, and for allowing us to dig a trench through the fault with their excavation equipment. The drivers, cooks and others involved in the 2004 fieldwork all contributed to a safe and enjoyable trip. B. Emmerson provided earthquake fault-plane solution data. E. Nissen provided useful comments on the manuscript. The final manuscript benefited from detailed and constructive reviews by D. Cunningham and J.-F. Ritz. Fieldwork was supported by the Keck Geology Consortium and the National Science Foundation. RTW is supported by NERC and the NERC-funded COMET research centre, and was supported in the field by a joint award (2004/R2-AS) from the Royal Society of London and the Mongolian Academy of Sciences.

References

Aitken, M.J., Bowman, S.G.E., 1975. Thermoluminescent dating: assessment of alpha particle contribution. Archaeometry 17, 132–138.

Badarch, G., Cunningham, D., Windley, B., 2002. A new terrance subdivision of Mongolia: implications for the Phanerozoic crustal growth of Central Asia. Journal of Asian Earth Sciences 21, 87–110.

Baljinnyam, I., Bayasgalan, A., Borisov, B.A., Cisternas, A., Dem'yanovich, M.G., Ganbaatar, L., Kochetkov, V.M., Kurushin, R.A., Molnar, P., Philip, H., Vashchilov, Yu.Ya., 1993. Ruptures of major earthquakes and active deformation in Mongolia and its surroundings. Geological Society of America, Memoir 181.

Bayasgalan, A., Jackson, J., Ritz, J.-F., Carretier, S., 1999a. 'Forebergs', flower structures, and the development of large intracontinental strike-slip faults: the Gurvan Bogd fault system in Mongolia. Journal of Structural Geology 21, 1285–1302.

Bayasgalan, A., Jackson, J., Ritz, J.-F., Carretier, S., 1999b. Field examples of strike-slip fault terminations in Mongolia and their tectonic significance. Tectonics 18, 349–411.

Bayasgalan, A., Jackson, J., McKenzie, D., 2005. Lithosphere rheology and active tectonics in Mongolia: relations between earthquake source parameters, gravity and GPS measurements. Geophysical Journal International 163, 1151–1179.

Calais, E., Vergnolle, M., San'kov, V., Lukhnev, A., Miroshnitchenko, A., Amarjargal, Sh., Deverchere, J., 2003. GPS measurements of crustal

deformation in the Baikal-Mongolia area (1994–2002): implications on current kinematics of Asia. Journal of Geophysical Research 108, doi:10.1029/2002JB002373.

Cunningham, W.D., 2000. Cenozoic normal faulting and regional doming in the southern Hangay region, Central Mongolia: implications for the origin of the Baikal rift province. Tectonophysics 331, 389–411.

Cunningham, D., 2005. Active intracontinental transpressional mountain building in the Mongolian Altai: defining a new class of orogen. Earth and Planetary Science Letters 240, 436–444.

Cunningham, W.D., Windley, B.F., Dorjnamjaa, D., Badamgarov, G., Saandar, M., 1996. A structural transect across the Mongolian Western Altai: active transpressional mountain building in central Asia. Tectonics 15, 142–156.

Cunningham, D., Dijkstra, A., Howard, J., Quarles, A., Badarch, G., 2003. Active intraplate strike-slip faulting and transpressional uplift in the Mongolian Altai. In: Storti, F., Holdsworth, R.E., Salvini, F. (Eds.), Intraplate Strike-Slip Deformation Belts. Geological Society, London, Special Publication 210, pp. 65–87.

Eberhart-Philips, D., et al., 2003. The 2002 Denali fault earthquake, Alaska: a large magnitude, slip-partitioned event. Science 300, 1113–1118.

Farr, T.G., Kobrick, M., 2000. Shuttle radar topography mission produces a wealth of data. Eos 81, 583–585.

Forman, S.L., Pierson, J., 2002. Late Pleistocene luminescence chronology of loess deposition in the Missouri and Mississippi river valleys, United States. Palaeogeography, Palaeoclimatology, Palaeoecology 186, 25–46.

Grunert, J., Lehmkuhl, F., Walther, M., 2000. Paleoclimatic evolution of the Uvs Nuur basin and adjacent areas (Western Mongolia). Quaternary International 65/66, 171–192.

Hanks, T.H., Kanamori, H., 1979. A moment magnitude scale. Journal of Geophysical Research 84, 2348–2350.

Khil'ko, S.D., Kurushin, R.A., Kochetkov, V.M., Balzhinnyam, I., Monkoo, D., 1985. Strong earthquakes, paleoseismological and macroseismic data. Earthquakes and the Bases for Seismic Zoning of Mongolia, Transactions 41 (The Joint Soviet-Mongolian Scientific Geological Research Expedition). Nauka, Moscow, pp. 19–83.

Kurushin, R.A., et al., 1997. The surface rupture of the 1957 Gobi–Altay, Mongolia, earthquake. Geological Society of America, Special Paper 320.

Lin, A., Fu, B., Guo, J., Zeng, Q., Dang, G., He, W., Zhao, Y., 2002. Co-seismic strike-slip and rupture length produced by the 2001 M_s 8.1 Central Kunlun earthquake. Science 296, 2015–2017.

Lehmkuhl, F., 1998. Quaternary glaciations in central and western Mongolia. Quaternary Proceedings 6, 153–167.

Molnar, P., Tapponnier, P., 1975. Cenozoic tectonics of Asia: effects of a continental collision. Science 189, 419–426.

Owen, L.A., Richards, B., Rhodes, E.J., Cunningham, W.D., Windley, B.F., Dorjnamjaa, D., Badamgarav, J., 1998. Relic permafrost structures in the Gobi of Mongolia: age and significance. Journal of Quaternary Science 13, 539–547.

Pan, B., Burbank, D., Wang, Y., Wu, G., Li, J., Guan, Q., 2003. A 900 k.y. record of strath terrace formation during glacial–interglacial transitions in northwest China. Geology 31, 957–960.

Poisson, B., Avouac, J.-P., 2004. Holocene hydrological changes inferred from alluvial stream entrenchment in North Tien Shan (Northwestern China). Journal of Geology 112, 231–249.

Philip, H., Megraoui, M., 1983. Structural analysis and interpretation of the surface deformations of the El Asnam earthquake of October 10, 1980. Tectonics 2, 17–49.

Philip, H., Rogozhin, E., Cisternas, A., Bousquet, J.C., Borisov, B., Karakhanian, A., 1992. The Armenian earthquake of 1988 December 7: faulting and folding, neotectonics and palaeoseismicity. Geophysical Journal 110, 141–158.

Prescott, J.R., Hutton, J.T., 1994. Cosmic ray contributions to dose rates for luminescence and ESR dating: large depths and long-term time variations. Radiation Measurements 23, 497–500.

Regard, V., Bellier, O., Thomas, J.-C., Bourles, D., Bonnet, S., Abbassi, M.R., Braucher, R., Mercier, J., Shabanian, E., Soleymani, Sh., Feghhi, Kh., 2005. Cumulative right-lateral fault slip across the Zagros-Makran transfer zone: role of the Minab-Zendan fault system in accommodating Arabia–Eurasia convergence in southeast Iran. Geophysical Journal International 162, 177–203.

Ritz, J.-F., Brown, E.T., Bourles, D.L., Philip, H., Schlupp, A., Raisbeck, G.M., Yiou, F., Enkhtuvshin, B., 1995. Slip rates along active faults estimated with cosmic-ray-exposure dates: application to the Bogd fault, Gobi–Altai, Mongolia. Geology 23, 1019–1022.

Rogozhin, E.A., Ovsyuchenko, A.N., Geodakov, A.R., Platonova, S.G., 2004. A strong earthquake of 2003 in Gornyi Altai. Russian Journal of Earth Sciences 5, 439–454.

Scholz, C.H., 1982. Scaling laws for large earthquakes: consequences for physical models. Bulletin of the Seismological Society of America 72, 1–14.

Tapponnier, P., Molnar, P., 1979. Active faulting and Cenozoic tectonics of the Tien Shan, Mongolia, and Baykal regions. Journal of Geophysical Research 84, 3425–3459.

Tomurtogoo, O., 2002. Tectonic Map of Mongolia. 1:1,000,000 Scale. Institute of Geology and Mineral Resources, Mongolian Academy of Sciences, Ulaanbaatar, Mongolia.

Vassallo, R., Ritz, J.-F., Braucher, R., Carretier, S., 2005. Dating faulted alluvial fans with cosmogenic ^{10}Be in the Gurvan Bogd mountain range (Gobi–Altay, Mongolia): climatic and tectonic implications. Terra Nova 17, 278–285.

Wells, D.L., Coppersmith, K.J., 1994. New empirical relationships among magnitude, rupture length, rupture width, rupture area, and surface displacement. Bulletin of the Seismological Society of America 84, 974–1002.

Yielding, G., Jackson, J.A., King, G.C.P., Sinvhal, H., Vita-Finzi, C., Wood, R.M., 1981. Relations between surface deformation, fault geometry, seismicity, and rupture characteristics during the El Asnam (Algeria) earthquake of 10 October 1980. Earth and Planetary Science Letters 56, 287–304.